Sprinkler irrigation droplet dynamics: a review and theoretical development

D. Zerihun and C.A. Sanchez

University of Arizona
Maricopa Agricultural Center
37860 West Smith-Enke Road
Maricopa, Arizona 85238

Annex to a report submitted to the USBR
February, 2014

Contents

List of Figures

Chapter 1. Introduction

In the context of sprinkler irrigation applications, droplet dynamics concerns the unsteady motion of water droplets through the ambient air, which could be quiescent (no-wind condition) or under steady uniform smooth horizontal motion itself (e.g. Fukui et al., 1980; Vories et al., 1987; Seginer et al., 1991; Carrion et a, 2001; Playan et al., 2009). Individual droplets are considered to be of constant size and shape throughout their motion, hence can be treated as rigid spheres in so far as their drag characteristics are concerned. Droplet motion is treated as an impulsively started motion at the sprinkler nozzle with known initial condition. The motion is curvilinear on the vertical plane, because of gravity. On the other hand, droplet motion on the horizontal plane is rectilinear, if the ambient air is quiescent or, it can be curvilinear if there is wind.

A sprinkler droplet dynamics model simulates the motion through the ambient air of individual droplets. The governing equation of droplet dynamics is a mathematical description of Newton's second law of motion (Fukui et al., 1980; von Bernuth and Gilley, 1984; Seginer, et al., 1991; Carrion, et al., 2001; Playan et al., 2009). The equation of motion relates the net unbalanced force acting on a water droplet, computed as the vector sum of the major forces acting on the droplet, with its acceleration (e.g., Shames, 1966; Soutas-Little and Inman, 1999). The resulting set of differential equations can then be solved numerically given the initial velocity and location of the particle (droplet) as it breaks away from the water jet, to determine its destination on the soil surface and its trajectory in a selected coordinate system.

The forces acting on a droplet include those that the ambient air exerts on the droplet and droplet weight. Forces exerted by the ambient air vary significantly in scale, are of different nature, and many of them may arise only under specific states of droplet motion relative to the ambient air. Hence, in subsequent discussions, first the forces that a quiescent ambient fluid (in this case air) exerts on a water droplet undergoing a steady or accelerated rectilinear motion are defined and their significance in the context of sprinkler irrigation droplet dynamics modeling is discussed. Based on which pertinent equations are derived. This will be followed by a discussion on the dynamics of an impulsively started, unsteady, motion of a water droplet through a quiescent ambient air. Then the more general case of the dynamics of the motion of a droplet undergoing unsteady three dimensional curvilinear motion under wind is discussed, the major forces acting on the droplet are defined and pertinent equations are derived. The discussion in this document is concluded with a derivation of the approximate equations used in the development of a sprinkler irrigation precipitation pattern simulation model reported in the companion document.

Chapter 2. Assumptions

The equations derived subsequently are based on the following set of assumptions:

1. Irrigation stream disintegrates into a range of water droplet diameters at the sprinkler nozzle;
2. The initial velocity of the droplets is equal to the average cross-sectional stream velocity at the nozzle, which is a function of sprinkler nozzle diameter and discharge;
3. The individual water droplets move through the ambient air independent of each other (without collision and the forces that the ambient air exert on droplets remain an affected by the motion of adjacent droplets);
4. Individual water droplets assume spherical shapes at emergence from the nozzle and remain spherical throughout their motion;
5. The diameters of the individual water droplets remain invariant throughout their motion (note that this should not imply that spray evaporation is neglected. Instead it is a statement of the fact that evaporation is not computed with a mechanistic model per individual droplets basis)
6. Under wind conditions, the ambient air in which the water droplets are fully immersed in is considered to be in a steady uniform horizontal flow with no velocity gradient in the vertical direction.

The rational basis for these assumptions, associated simplifications, and the limitations they impose on the predictive capability of the model as regards precipitation distribution, and hence irrigation application rate, about a sprinkler are discussed in the companion document (Zerihun and Sanchez, 2014). Overall, the implications of these assumptions for sprinkler irrigation droplet dynamics are: the initial conditions for droplet motion are established, droplets are treated as rigid spheres with constant diameter and shape throughout their motion. The dynamics of the complex process of the simultaneous motion of a system of particles (which involves direct interaction between particles and indirect interaction through their effect on the ambient air) can be reduced to the dynamics of the motion of individual particles. Wind is considered as a steady uniform horizontal air flow.

Chapter 3. Forces that a quiescent ambient air exerts on a water droplet undergoing steady or accelerated rectilinear motion

In this section the type of forces that a quiescent ambient air exerts on a water droplet undergoing a steady or accelerated rectilinear motion are described. Equations relating aerodynamic drag (under steady state motion) or the aggregate effects of the major forces acting on the droplet (under conditions of accelerated droplet motion) with pertinent variables are presented. Note that the simplifying assumptions, as regards droplet size and shape, listed above are considered applicable here.

3.1 Steady motion of water droplet

The simplest type of water droplet motion consists of one in which a droplet moves at a constant velocity in a straight line (rectilinear motion) through a quiescent air. In such a case, the forces exerted by the ambient air on the droplet consist of drag force, buoyancy, and lift force (Vennard, 1941; Granger, 1995). However, buoyant force on the water droplet is considered negligible and the lift force is ignored in sprinkler droplet dynamics application, apparently on accounts of symmetry of the spherical droplets. The drag force is composed of two types of forces: the friction drag, which accounts for the tangential shear stress on the droplet surface, and the pressure drag (form drag), representing the normal stresses on the droplet surface. The relative magnitudes of the contributions of friction drag and pressure drag to the total drag is given as a function of the Reynolds number, Re. At low droplet Reynolds numbers ($Re < 1.0$), the fluid glides smoothly over the surface of the droplet covering it fully and hence friction drag predominates (Vennard, 1941; Granger, 1995). In the range $1.0 < Re \leq 1000$, a recirculation region (turbulent wake) began to form and grow behind the droplet. In which case, the contribution of friction drag becomes increasingly less important and the effect of pressure drag tends to be the dominant form of drag. In the range 1000<*Re* the wake behind the droplet stabilizes. Experience with simulation results suggests that, water droplet *Re* in sprinkler applications is typically less than 10^4. In sprinkler irrigation modeling applications, the term drag force typically refers to the combined effect of these two components on a water droplet without any distinction.

In light of the assumptions outline above, water droplets in the context of sprinkler irrigation droplet dynamics modeling can be treated as solid spheres in so far as their shapes and sizes are concerned. In addition, considering the relatively low velocities (about 30.0m/s or less) common in sprinkler droplet dynamics, the effect of changes in the ambient air density due to compression and its effect on drag can be considered negligible. With this consideration in place, the modulus of the drag force, *D*, that the ambient air exerts on a water droplet undergoing a steady motion can be considered to be a function of four physical quantities: the density, ρ, and viscosity, μ, of the ambient air, droplet diameter, *d*, and droplet relative velocity with respect to the ambient air, V_r. Note that these parameters take into account the fact that drag has both pressure and friction components and that it is a function of the geometry and relative motion of the droplet with respect to the ambient air. Considering that the ambient air is assumed to be stationary, V_r is equal to the absolute velocity of the droplet. The functional relationship between the dependent variable, *D*, and the independent variables (ρ,μ,d,V_r) can be expressed as:

$$f(D,\rho,\mu,d,V_r) = 0 \tag{1}$$

In Eq. 1, there are five physical quantities expressed in terms of the three fundamental dimensions of mass *[M]*, length *[L]*, and time *[T]*:

$$[D] = \frac{ML}{T^2},\quad [\rho] = \frac{M}{L^3},\quad [\mu] = \frac{M}{LT},\quad [d] = L,\quad [V_r] = \frac{L}{T} \tag{2}$$

In Eq. 2, [.] = the dimension of a physical quantity. Using the Buckingham π theorem, Eq. 1. can be expressed as a relationship between two dimensionless products (π_1,π_2):

$$f(\pi_1,\pi_2) = 0 \tag{3}$$

where

$$\pi_1 = \frac{D}{\rho d^2 V_r^2} \quad and \quad \pi_2 = \frac{\mu}{\rho V_r d} = \frac{1}{Re} \qquad (4)$$

The physical and mathematical principles underlying the Buckingham π theorem are described by Langhaar (1980). With the drag force, D, as the dependent variable, Eq. 2 can be given as the product of a dimensionless constant, C, some function of the Reynolds number, and an expression of the form, $\rho d^2 V_r^2$:

$$D = Cf(Re)(\rho d^2 V_r^2) \qquad (5)$$

In Eq. 5, if the dimensionless constant $C = \pi/8$, the equation for aerodynamic drag, D, acting on a droplet undergoing steady rectilinear motion in otherwise quiescent viscous fluid results:

$$D = C_{ds} A \frac{\rho}{2} V_r^2 \qquad (6)$$

where C_{ds} = the steady state drag coefficient which is a function of the droplet Re *[-]* and A = the projected area of the sphere (L^2). Noting that $\rho V_r^2/2$ is equivalent to the pressure that the ambient air exerts on a droplet and that the product of this expression with the projected area of the droplet yields pressure force acting on the droplet, it then follows that the expression in Eq. 6 approximates the overall drag force on the droplet as the product of the steady state drag coefficient and the pressure force that the ambient air exerts on the droplet. For rigid sphere undergoing steady motion at low Re (≤1.0), the equation relating steady state drag coefficient with Re is determined theoretically (e.g., Vennard, 1941; Granger, 1995). However, for $1.0<Re$ the relationship between C_{ds} and Re was determined experimentally (Temkin and Kim, 1980). The steady state drag coefficient, C_{ds}, decreases as Re increases in the range $Re \leq 1000$ and remains constant at about $C_{ds} = 0.45$ in the range $1000<Re$. Note that the individual droplets in sprinkler irrigation droplet dynamics modeling are essentially treated as rigid spheres, hence the standard $C_{ds}(Re)$ relationship should be applicable.

3.2 Unsteady motion of water droplet

For water droplets moving through air steady state motion is an uncommon occurrence. It is often described in relation to rain water droplets that have accelerated to terminal velocities, before reaching the ground surface (Laws, 1941) and in situations where the droplets are fully carried by steadily moving air with no relative motion between the ambient air and droplet (Temkin, and Mehta, 1982). Droplets (often small diameter droplets) from a sprinkler water jet decelerating under the action of drag may, in the course of the latter part of their motion, be fully carried by wind. However, in sprinkler modeling applications the motion of water droplets (solid spheres) through the ambient air is typically unsteady.

Theoretical and experimental studies into the effect of unsteady motion of droplets fully immersed in a quiescent fluid shows that at any given moment during their motion, the magnitude and nature of forces that the fluid exerts on the droplet differ from the steady state drag force (Odar and Hamilton, 1964; Karanfilian and Kotas, 1978; Aggarwal and Peng, 1995). Note that while some of these studies are based on experiments involving the motion of solid spheres fully immersed in oil, given the assumptions introduced above with regard to the size and shape of droplets and the properties of the ambient fluid, their inferences are generally considered applicable to droplet motion through air (e.g., Aggarwal and Peng, 1995). Overall, the forces exerted by the ambient fluid are considered to be composed of three components: the steady state drag force expressed as a function of the instantaneous Reynolds number, Eq. 6; force related to the instantaneous acceleration (with a form of droplet mass times acceleration); and force expressed in terms of a time integral representing the acceleration history of the droplet – which could be attributed to the disturbances that prior droplet motion has introduced to the ambient fluid.

The form of the equation describing these forces and its parameters are well defined at low Reynolds number, $Re \leq 1.0$, however, at moderate to high Reynolds number the values of the model parameters are not well defined (Karanfilian and Kotas, 1978; Aggarwal and Peng, 1995). Hence, because of the uncertainty in parameter estimates and also on accounts of the complexity of the equation and applicable numerical solutions, a simpler formulation based on Eq. 6 is often used to approximate the aggregate effects of steady drag force and the forces arising due to acceleration. Such an approach is described as the correlation approach (e.g. Aggarwal and Peng, 1995). With this approach the steady state drag coefficient, in Eq. 6, is replaced with a parameter often termed as the unsteady drag coefficient, C_{du}; which has been shown to be a function the instantaneous *Re* and the acceleration number, a_n (Karanfilian and Kotas, 1978; Aggarwal and Peng, 1995).

$$D = C_{du}(Re, a_n)A\frac{\rho}{2}V_r^2 \qquad (7)$$

where *D* = the modulus of the drag force *[ML/T²]*. The acceleration number is, a dimensionless physical quantity, used to measure the relative strengths of the droplet convective acceleration to its local acceleration and is defined as (Karanfilian and Kotas, 1978; Temkin and Kim, 1980):

$$a_n = \frac{a_r d}{V_r^2} \quad where \quad a_r = \frac{dV_r}{dt} \qquad (8)$$

where a_r = the relative acceleration *(L/T^2)*. The correlation approach has been shown to provide a good fit between the computed and measured data describing the accelerated motion of solid spheres fully immersed in oil (Karanfilian and Kotas, 1978). Temkin and Kim (1980) have used the correlation approach to fit measured data from an experiment conducted under laboratory condition, in which spherical water droplets undergo accelerated motion through air which also moves, but with a uniform velocity. Finally, to the extent that the forces exerted by the ambient air on a water droplet, undergoing unsteady motion, are approximated with a form of the drag equation (through modifications introduced to the steady drag coefficient), they will not be explicitly considered in subsequent analysis.

Chapter 4 Dynamics of droplet motion through a quiescent ambient air

In order to facilitate ease of visualization of droplet motion and the kind and nature of forces acting on droplet the three dimensional droplet trajectory, associated velocity, and acceleration vectors are presented and discussed in terms of their projections on the horizontal and vertical planes. However, the derivation of equations is based on vector algebra in a rectangular coordinate system.

4.1 Description of droplet motion including trajectory, velocity, and acceleration components

The discussion in this section concerns the dynamics of an impulsively started unsteady droplet motion through a quiescent ambient air, which is a special case of an accelerated motion of water droplet through a viscous fluid. An assumed trajectory of the water droplet, its initial conditions, and landing coordinates on the irrigated field surface are shown in Figure 1a, with the origin of the coordinate system set at the intersection of the centerlines of the sprinkler riser pipe and the lateral (assuming the lateral is horizontal and the riser is vertical). Figures 1b and 1c depict the droplet initial absolute velocity vector, $\boldsymbol{V_0}$, and the absolute velocity vector at some time, *t*, following its release from the sprinkler nozzle, and their components along the coordinate axes.

A closer look at the projections of the water droplet trajectory on a horizontal and vertical plane reveals some interesting features of the nature of accelerated droplet motion through an otherwise quiescent ambient air condition (Figure 2a). It can be noted from Figures 2a and 2b that the projected droplet trajectory on the vertical plane is curvilinear (due to gravity), implying that droplet acceleration vector on the vertical plane has both tangential and normal components to the trajectory (e.g., Shames, 1966; Soutas-Little and Inman, 1999). The tangential component, $\boldsymbol{a}_{vt}$ (which does not include the component of gravitational acceleration tangent to the droplet trajectory), represents the change in the magnitude of droplet absolute velocity on the vertical plane. The normal component, on the other hand, accounts for the change in direction of the projection of droplet absolute velocity vector on the vertical plane. Hence, it is responsible for the curvilinear motion there. For reason of simplicity of notion, the normal component of acceleration on the vertical plane is not shown in Figure 2b. However, it can readily be noted that it is a component of the gravitational acceleration normal to droplet trajectory.

The projection of droplet trajectory on the horizontal plane is a straight line and the angle that it makes with the *x*- and *y*- coordinate axes is set by the horizontal angular setting of the sprinkler nozzle with respect of a reference axis (the *x*-axis), θ_{hx0}, at the time droplet leaves the sprinkler nozzle (Figure 2a). The fact that the projection of the droplet trajectory on the horizontal plane is straight-line implies that droplet acceleration on the horizontal plane, $\boldsymbol{a}_h$, is entirely due to changes in the magnitude of the projected droplet absolute velocity vector on the horizontal plane (alternatively stated, the normal component of acceleration on the horizontal plane is zero). It also indicates that droplet velocity, acceleration, and force vectors lie on the same vertical plane. Hence, droplet motion is planar (it is two-dimensional on a vertical plane)

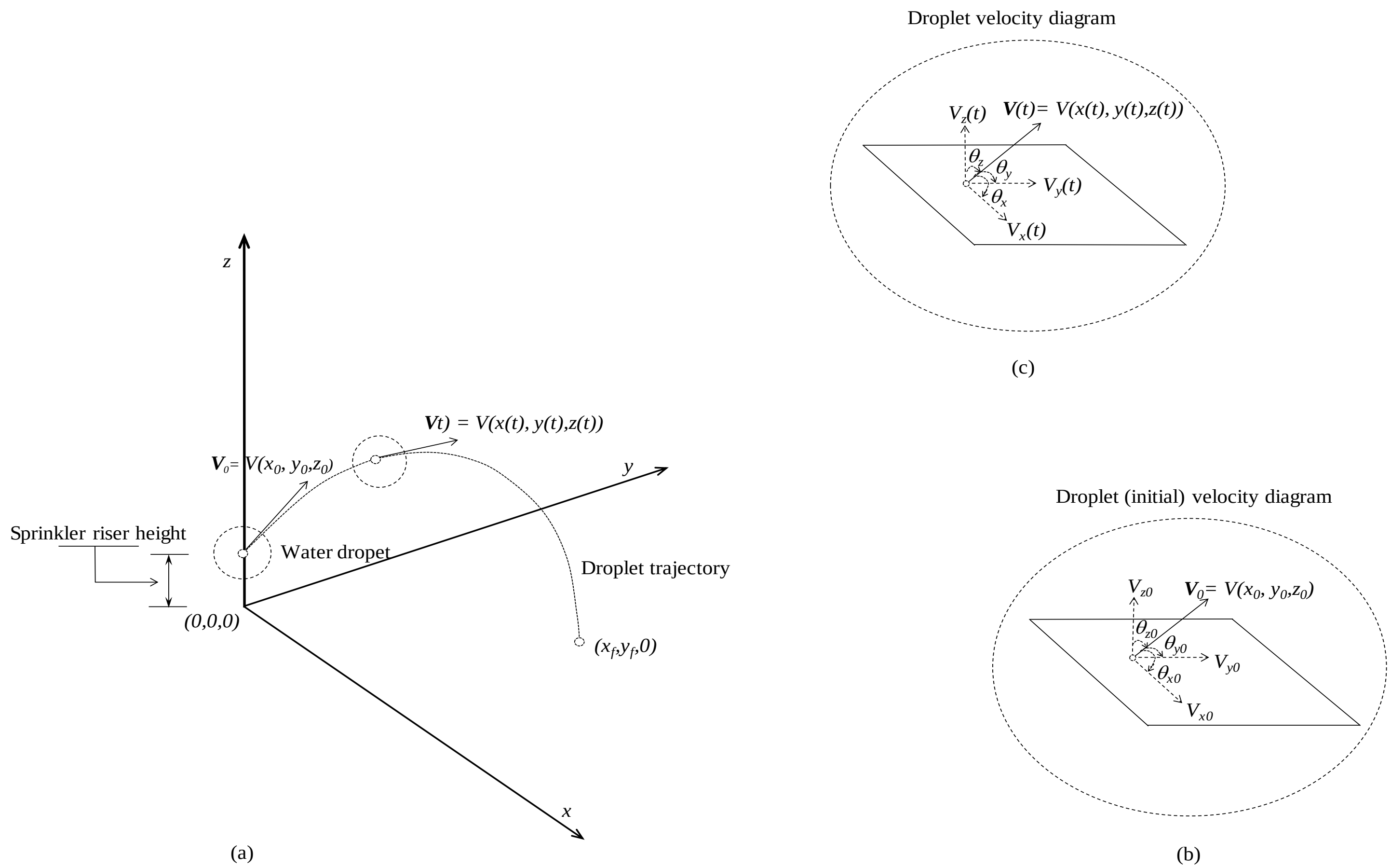

Figure 1 (a) Sprinkler irrigation droplet trajectory and droplet absolute velocity vectors; (b) Initial velocity vector, $\boldsymbol{V}_0$,(L/T), its components, and (c) Velocity vector at time t, $\boldsymbol{V}(t)$, following the release of droplet from sprinkler nozzle, and its components (where V_{x0}, V_{y0}, and V_{z0} = the components of droplet initial velocity vector along the x, y and z coordinate axes, respectively; x_0, y_0, and z_0 = the components of the droplet position vector along the coordinate axes at time $t=0$; $V(x(t)),V(y(t))$, and $V(z(t))$ = the components of droplet absolute velocity vector along the respective coordinate axes at time t; θ_x, θ_y, and θ_z = the angle that the instantaneous velocity vector, $\boldsymbol{V}(t)$, makes with the coordinate axes; x_f, y_f, and z_f = droplet landing coordinates on the field surface) and the vertical plane of motion is completely defined by the angular setting of the sprinkler nozzle at the time droplet departs the sprinkler nozzle. Note that this has an important implication in the numerical solution of the droplet dynamics equations. While the above discussion helps visualize the effect of wind on droplet motion, eventually a quantitative description of wind effects on droplet motion has to be presented in a three dimensional coordinate system (Figure 3d).

4.2 Major forces acting on a droplet

Droplet acceleration in a given direction is proportional to the net unbalanced force on the droplet in that same direction. Hence, the above description of droplet acceleration components can be used to define the corresponding forces acting on the droplet. It can readily be noted that droplet weight, $\boldsymbol{F}_w$, which is directly proportional to gravitational acceleration, g, is one of the forces that acts on the droplet (Figure 2b). It then follows from the preceding discussion that the droplet tangential acceleration, in three dimensions, $\boldsymbol{a}_t$ (which is a function of $\boldsymbol{a}_h$ and $\boldsymbol{a}_{vt}$) is evidently related to the attenuation of droplet velocity due to aerodynamic drag, $\boldsymbol{D}$. The relationship between the major forces acting on a droplet, consisting of aerodynamic drag, $\boldsymbol{D}$, and droplet weight, $\boldsymbol{F}_w$, is depicted in Figure 2d.

4.3 Equations of droplet dynamics under no-wind condition

From Newton's second law of motion at any given time in the course of droplet motion, the vector sum of forces acting on a droplet can be related to the droplet acceleration vector as follows:

$$m\boldsymbol{a} = \sum \boldsymbol{F} \qquad (9)$$

where m = droplet mass $[M]$, $\boldsymbol{a}$ = droplet acceleration vector $[L/T^2]$, $\boldsymbol{F}$ = force vector $[ML/T^2]$, and the expression $\sum \boldsymbol{F}$ represents the vector sum of the forces acting on the droplet. Note that in subsequent discussion, following convention, bold face letters are used to define vectors.

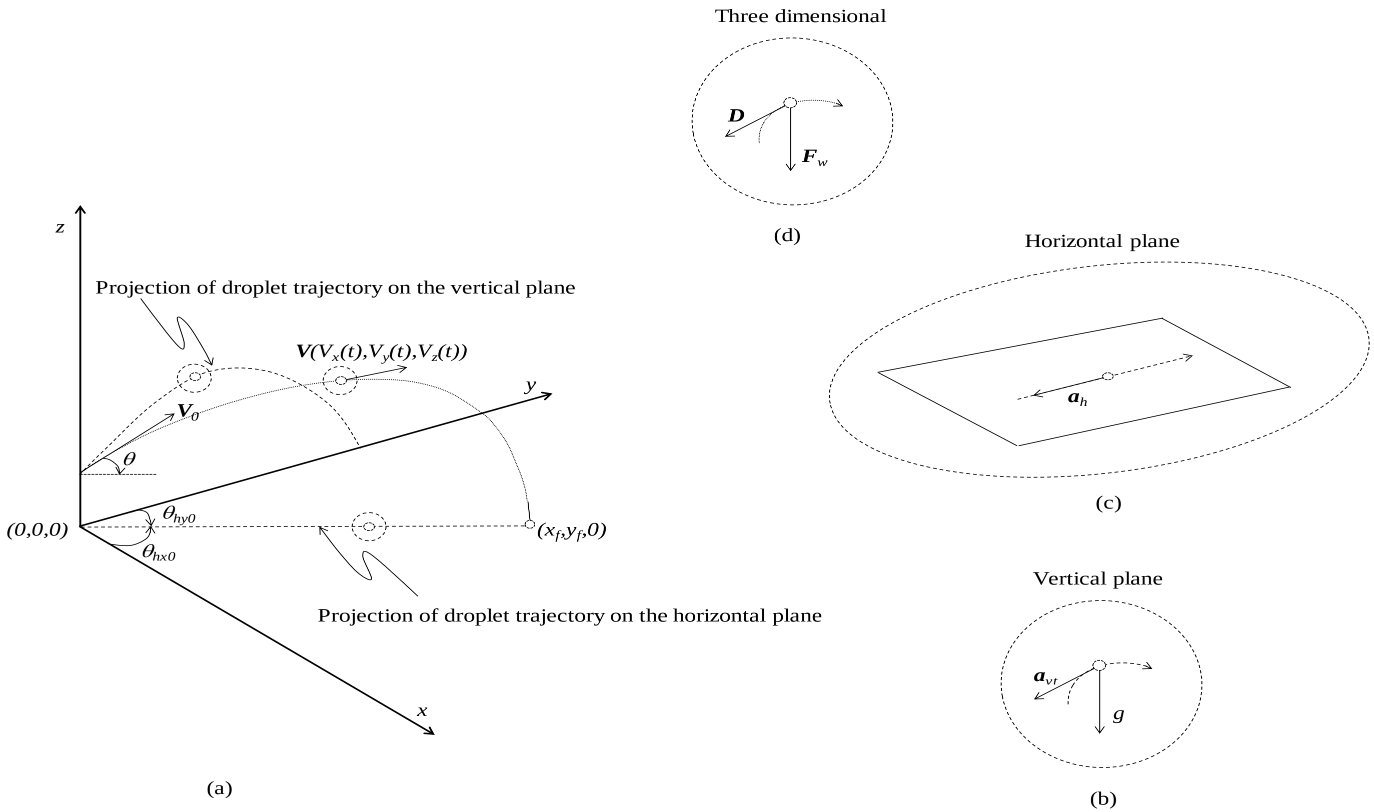

Figure 2 (a) Assumed droplet trajectory in a rectangular coordinate system, instantaneous droplet absolute velocities, and projections of droplet trajectory on a horizontal and a vertical plane under conditions of no-wind; (b) Projections of droplet instantaneous acceleration on a vertical plane; (c) Projection of droplet instantaneous acceleration on a horizontal plane; and (d) Droplet free-body diagram (where θ = the angle that the initial droplet absolute velocity vector, $\boldsymbol{V}_0$, makes with a horizontal plane; θ_{hx0} = the horizontal angular setting of the sprinkler nozzle at the time droplet leaves the nozzle (also equal to the angle that the projection of the initial droplet absolute velocity vector on the horizontal plane makes with the *x*-axis); θ_{hy0} = the angle that the projection of the droplet initial velocity vector on the horizontal plane makes with the *y*-axis; $\boldsymbol{a}_{vt}$ = the projection of droplet tangential acceleration on a vertical plane, excluding the component of gravitational acceleration $[L/T^2]$; g = gravitational acceleration $[L/T^2]$ and $\boldsymbol{a}_h$ = projection of droplet tangential acceleration on a horizontal plane $[L/T^2]$, $\boldsymbol{D}$ = drag force $[ML/T^2]$, and $\boldsymbol{F}_W$ = droplet weight $[ML/T^2]$)

Using a rectangular coordinate system, at any given time, *t*, droplet acceleration vector, ***a****(t)*, can be expressed as

$$\boldsymbol{a} = \frac{d^2\boldsymbol{r}}{dt^2} = \frac{d^2x}{dt^2}\boldsymbol{i} + \frac{d^2y}{dt^2}\boldsymbol{j} + \frac{d^2z}{dt^2}\boldsymbol{k} \qquad (10)$$

where ***r****(t)* = the water droplet position vector

$$\boldsymbol{r}(t) = x(t)\boldsymbol{i} + y(t)\boldsymbol{j} + z(t)\boldsymbol{k} \qquad (11)$$

and *x(t)*, *y(t)*, and *z(t)* are the coordinates of the droplet along the *x*, *y*, and *z* axes at time, *t*, and ***i***, ***j***, and ***k*** are unit vectors, along the three coordinate axes, given as

$$\boldsymbol{i} = (1,0,0), \quad \boldsymbol{j} = (0,1,0), \quad and \quad \boldsymbol{k} = (0,0,1) \qquad (12)$$

In Eq. 10 $\frac{d^2x}{dt^2}$, $\frac{d^2y}{dt^2}$, and $\frac{d^2z}{dt^2}$ are the components of $\boldsymbol{a} = (a_x, a_y, a_z)$ along the coordinate axes, respectively.

The vector sum of the forces acting on the droplet (Figure 2d) can be expressed as

$$\sum \boldsymbol{F} = \boldsymbol{D} + \boldsymbol{F}_w \qquad (13)$$

In what follows expressions in vector form for the drag, ***D***, and droplet weight, $\boldsymbol{F}_w$, forces will be presented.

Drag force, D: The drag force that the ambient air exerts on the droplet has the same line of action as the droplet relative velocity vector, $\boldsymbol{V}_r$ (referenced with respect to the ambient air); but acts in opposite direction to it. It then follows from vector algebra (e.g., Ellis and Gulick, 1991) that the equation for the drag force vector can be obtained by multiplying Eq. 7 by the negative of a unit vector, $\boldsymbol{e}_v$, which has the same line of action but opposite sense as $\boldsymbol{V}_r$

$$\boldsymbol{D} = -C_{du} A \frac{\rho}{2} |\boldsymbol{V}_r| |\boldsymbol{V}_r| \boldsymbol{e}_v \qquad (14)$$

In Eq. 14, $|\boldsymbol{V}_r|$ = the modulus of the instantaneous droplet relative velocity vector, and by definition the unit vector along $\boldsymbol{V}_r$ is given as $\boldsymbol{e}_v = \frac{\boldsymbol{V}_r}{|\boldsymbol{V}_r|}$. The vector form of the drag equation for a droplet undergoing unsteady motion (Figure 2a) through an otherwise quiescent air can then be expressed as

$$\boldsymbol{D} = -C_{du} A \frac{\rho}{2} |\boldsymbol{V}_r| \boldsymbol{V}_r \quad (15)$$

Noting that wind velocity is considered zero, the droplet relative velocity with respect to the ambient air, $\boldsymbol{V}_r$, is the same as the droplet absolute velocity vector, $\boldsymbol{V}$. Nonetheless, in subsequent derivation the notation $\boldsymbol{V}_r$ is retained in order to emphasize the significance of $\boldsymbol{V}_r$ in drag computation. Hence, the vector equation for $\boldsymbol{V}_r$ in rectangular coordinate system can be given as

$$\boldsymbol{V}_r = V_x \boldsymbol{i} + V_y \boldsymbol{j} + V_z \boldsymbol{k} \quad (16)$$

where V_x, V_y, and V_z = the components of droplet absolute velocity along the coordinate axes (Figure 1). Substituting Eq. 16 in Eq. 15 yields the vector equation for the drag force acting on a droplet undergoing unsteady motion in a quiescent air

$$\boldsymbol{D} = -C_{du} A \frac{\rho}{2} |\boldsymbol{V}_r| \left(V_x \boldsymbol{i} + V_y \boldsymbol{j} + V_z \boldsymbol{k} \right) \quad (17)$$

Droplet weight, $\boldsymbol{F}_w$: Noting that at any given point along the trajectory of the water droplet, the droplet weight is directed in the negative z direction (Figure 2d), the vector form of the equation for $\boldsymbol{F}_w$ is given as

$$\boldsymbol{F}_w = -mg\boldsymbol{k} \quad (18)$$

Substituting Eqs. 17, 18, and 10 in Eq. 9, yields the vector differential equation (in a rectangular coordinate system) describing accelerated (unsteady) motion of a droplet through an otherwise quiescent air

$$m\left(\frac{d^2x}{dt^2}\boldsymbol{i}+\frac{d^2y}{dt^2}\boldsymbol{j}+\frac{d^2z}{dt^2}\boldsymbol{k}\right)=-C_{du}A\frac{\rho_a}{2}\left|\boldsymbol{V}_r\right|\left(V_x\boldsymbol{i}+V_y\boldsymbol{j}+V_z\boldsymbol{k}\right)-mg\boldsymbol{k} \qquad (19)$$

noting that

$$\frac{dV_x}{dt}=\frac{d^2x}{dt^2}, \quad \frac{dV_y}{dt}=\frac{d^2y}{dt^2}, \quad and \quad \frac{dV_z}{dt}=\frac{d^2z}{dt^2} \qquad (20)$$

subject to the condition

$$V_x=\frac{dx}{dt}, \quad V_y=\frac{dy}{dt}, \quad and\ V_z=\frac{dz}{dt} \qquad (21)$$

The scalar form of the equation of motion, Eq. 19, along the three coordinate axes can then be given in terms of six equations with six variables:

$$\frac{dV_x}{dt}=-\xi C_{du}\left|\boldsymbol{V}_r\right|V_x \qquad (22)$$

$$\frac{dx}{dt}=V_x \qquad (23)$$

$$\frac{dV_y}{dt}=-\xi C_{du}\left|\boldsymbol{V}_r\right|V_y \qquad (24)$$

$$\frac{dy}{dt}=V_y \qquad (25)$$

$$\frac{dV_z}{dt}=-\xi C_{du}\left|\boldsymbol{V}_r\right|V_z-g \qquad (26)$$

$$\frac{dz}{dt}=V_z \qquad (27)$$

Noting that the mass of the water droplet, *m*, and its projected area normal to the direction of motion, *A*, are given as:

$$m=\frac{\pi\rho_w}{6}d^3 \quad and \quad A=\frac{\pi}{4}d^2 \qquad (28)$$

where π = the ratio of the circumference of a circle to its diameter *[-]* and ρ_w = the density of water *[ML/T^2]*, in Eqs. 22-27

$$\xi = \frac{3}{4}\left(\frac{\rho}{\rho_w}\right)\left(\frac{1}{d}\right) \tag{29}$$

Equations 22-27, represent a coupled system of (six) first-order nonlinear differential equations with six unknowns (V_x, V_y, V_z, x, y, z). Problem definition is completed with the statement of initial conditions. Considering the intersection of the centerlines of the lateral and sprinkler riser pipes as the origin of the coordinate system, the initial conditions can be given as:

$$\left.\begin{array}{l} x(t=0) = 0.0, \quad y(t=0) = 0.0, \quad z(t=0) = z_0 \\ V_x(t=0) = V_{x0} = |\mathbf{V}_0| cos(\theta_{x0}), \quad V_y(t=0) = V_{y0} = |\mathbf{V}_0| cos(\theta_{y0}) \\ V_z(t=0) = V_{z0} = |\mathbf{V}_0| cos(\theta_{z0}) \end{array}\right\} \tag{30}$$

In Eq. 30, z_0 = sprinkler riser pipe height *(L)*, $|\mathbf{V}_0|$ = the magnitude of the initial droplet absolute velocity vector *(L)* and can be computed based on measured or computed sprinkler discharge and nozzle diameter, and θ_{x0}, θ_{y0}, and θ_{z0} = the angles that initial droplet absolute velocity vector makes with the coordinate axes. Considering a counter clockwise sprinkler rotation referenced from the positive *x*-axis (Figure 3a), the sprinkler nozzle angular setting, θ_{hx0}, is known. The sprinkler vertical tilt angle, θ, is also a known quantity for a given sprinkler model. Then the quantities θ_{x0}, θ_{y0}, and θ_{z0} can be computed with

$$\left.\begin{array}{l} \theta_{x0} = a\,cos\left(cos(\theta)\, cos(\theta_{hx0})\right), \quad \theta_{y0} = a\,cos\left(cos(\theta)\, sin(\theta_{hx0})\right) \\ and \\ \theta_{z0} = \frac{\pi}{2} - \theta \end{array}\right\} \tag{31}$$

The vector differential equation, Eq. 19, or its scalar counterparts, Eqs. 22-27, constitute the basic equations describing droplet dynamics in the context of sprinkler irrigation applications, for the conditions in which wind velocity can be considered zero (Fukui et al., 1980; Vories et al., 1987; Seginer et al., 1991; Carrion et al., 2001; Playan et al., 2009). The coupled system of equation, Eqs. 22-27, along with pertinent initial conditions, Eq. 30, represent an initial value problem that can be solved numerically using established methods (Burden et al., 1981; Press et al., 1997; Matthews et al., 2004).

Chapter 5 Dynamics of droplet motion under wind

5.1 Description and assumptions pertaining to wind

Operating sprinkler irrigation systems under quiescent atmospheric conditions are considered ideal from the stand point of attaining high irrigation uniformity under overlapped field conditions. In practice, however, sprinkler irrigation is often conducted under windy conditions. In sprinkler droplet dynamics applications wind is considered as a smooth (streamlined), steady uniform horizontal air flow, with no vertical component. The section of the atmosphere in which the motion of sprinkler droplets takes place is the surface layer where boundary layer effects are significant, and hence vertical gradients in the horizontal wind velocity vector can be significant (Arya, 1988). Although a logarithmic wind profile equation can be used to estimate vertical variations in wind velocity, explicit consideration of these variations in the droplet dynamics model at least conceptually implies the presence of sheared flow and contradicts the streamlined tranquil horizontal air flow assumed above. In addition, if horizontal wind velocities are considered variable with height above the field surface, during numerical computations at each time step wind velocity (instead of being a constant input) needs to be computed as a function of the vertical coordinate of the droplet, which is determined as part of the numerical solution for the time step. This complicates the numerical solution by requiring an iterative procedure during each time step. Hence, the approach adopted here assumes that wind is a steady uniform horizontal air flow with no velocity gradient in the vertical direction. Hence, in effect the wind velocity vector considered here is an effective average wind velocity over the duration of irrigation in the surface layer where water droplet motion takes place.

Early approaches to modeling wind effects on sprinkler droplet dynamics and precipitation pattern distribution (Fukui et al., 1980; von Bernuth and Gilley, 1984; Vories et al., 1987) were based on the assumption that equations of the form given in Eqs. 22-27 can be used to take into account the effect of wind on drag and droplet drift, with $\boldsymbol{V}_r$ computed as the droplet relative velocity with respect to the velocity of the ambient air (wind velocity). However, such an approach was found to be inadequate to represent the distortions that wind introduces in the participation pattern about a sprinkler. Commonly used modifications in order to take into account wind effects, on droplet motion and sprinkler precipitation pattern, more effectively involves empirical approximations of the unsteady drag coefficient as a function of the steady drag coefficient and trigonometric terms implicitly accounting for drag and droplet drift effects (Seginer et al., 1991; Carrion et al., 2001; Playan et al., 2009). However, in the following discussion a system of equations will be derived based on a more rigorous physical reasoning, taking into account the type of motion and the nature of the corresponding forces that wind introduces into the dynamics of droplet motion (compared to droplet motion under an equivalent quiescent ambient air condition). As will be shown subsequently, an important feature of the approach presented here, as distinct from earlier approaches, is the way the effect of wind on droplet motion is taken into account. In stead of simply encapsulating wind effects into the droplet relative velocity vector, $\boldsymbol{V}_r$, in the current approach wind velocity vector is resolved into components along and normal to the droplet absolute velocity vector. Then the tangential and normal components of the wind velocity vector, which are vectors themselves in a fixed rectangular coordinate system, are shown to be representing wind effects on drag and droplet drift, respectively. Based on which a mathematical expression for droplet drift would be defined and incorporated into the equation of motion.

Wind drift effect in the context of sprinkler irrigation is often described as wind induced distortions on sprinkler irrigation precipitation pattern relative to that associated with an equivalent no-wind condition. However, the concept of droplet wind drift can be more subtle. Although in principle, any wind induced deviation in droplet trajectory (which could have both horizontal and vertical components) from an equivalent no-wind condition can be considered droplet wind drift, in subsequent development only those that can be attributed to the radial forces introduced by wind are considered as wind drift.

5.2 Description of droplet trajectory, acceleration vector, and its components

In order to conceptualize the effect of wind on droplet motion, initially consider a scenario in which a droplet undergoes an impulsively started accelerated motion in a quiescent ambient air condition under a given set of conditions: air viscosity, density, droplet diameter, sprinkler design factors, nozzle coordinates, and pressure head at sprinkler nozzle. Then at some time *t* following the release of the droplet from the sprinkler nozzle, assume a steady uniform wind vector, ***W*** (not parallel to the absolute velocity vector of the droplet), is spontaneously imposed on it (Figure 3a). Consistent with the preceding description of droplet motion through a quiescent air (Section 4), in the first part of droplet motion the projected droplet trajectory on the horizontal plane would be a straight line. However, with the introduction of wind, intuitive physical reasoning, and observations of actual field irrigation events, suggest that the projection of droplet trajectory on the horizontal plane would begin to veer out of the rectilinear path that it followed during the initial phase of its motion. Droplet trajectory on the horizontal plane will continue to change direction with time until either the wind velocity vector and the droplet absolute velocity vector lie on the same vertical plane (i.e., the wind velocity vector and the projection of the droplet absolute velocity vector on the horizontal plane, $\boldsymbol{V}_h$, become collinear) or the droplet reaches it destination on the surface of the irrigated field (Figure 3a).

The preceding implies that, under wind, the projection of droplet trajectory on the horizontal plane also represents curvilinear motion. In which case, droplet acceleration in the horizontal plane has both tangential, $\boldsymbol{a}_{ht}$, and normal, $\boldsymbol{a}_{hn}$, components (Figure 3b). Evidently, the tangential acceleration component is related to the attenuation of the droplet absolute velocity vector projected on the horizontal plane as affected by aerodynamic drag (taking into account wind effects). On the other hand, the normal component of acceleration is responsible for the change in direction of the droplet absolute velocity vector and hence for the curvilinear motion of droplet on the horizontal plane. The fact that the normal acceleration component and the associated curvilinear motion arise with the introduction of wind suggests that the component of wind velocity normal to droplet trajectory, on the horizontal plane, is in some form related to the normal acceleration. Clearly the preceding discussion, based on analyses of droplet motion and related acceleration components ($\boldsymbol{a}_{ht}$ and $\boldsymbol{a}_{hn}$), shows that the effect of wind on droplet motion (as

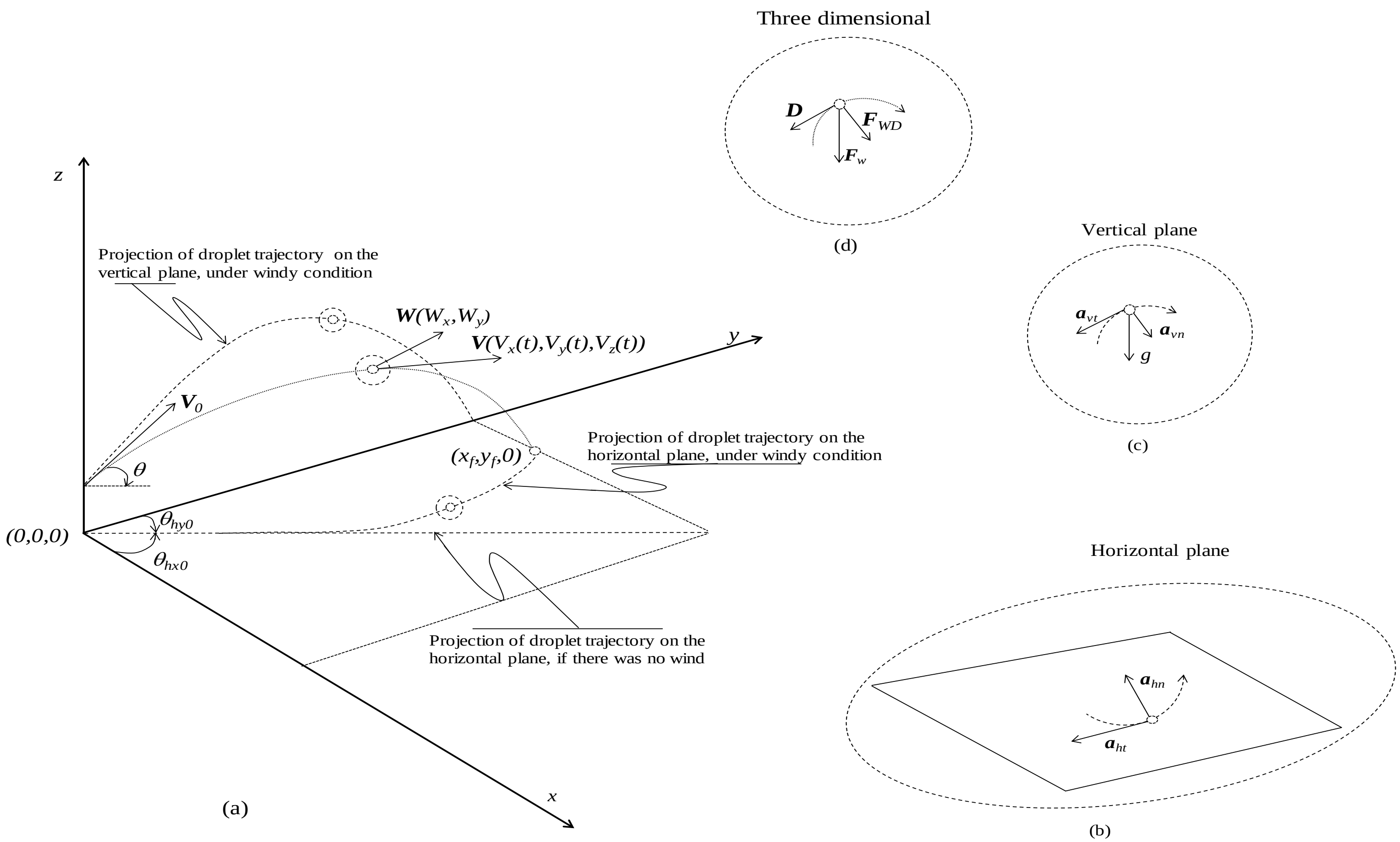

Figure 3 (a) Assumed droplet trajectory in a rectangular coordinate system, instantaneous droplet absolute velocities, and projections of droplet trajectory on a vertical and a horizontal plane under conditions of a steady uniform horizontal wind, (b) The projection of droplet instantaneous acceleration on a horizontal plane, (c) Projection of droplet instantaneous acceleration on a vertical plane, and (d) Droplet free-body diagram (where $\boldsymbol{a}_{ht}$ and $\boldsymbol{a}_{hn}$ = projections on a horizontal pane of the tangential and normal components of droplet acceleration, respectively (L/T^2); $\boldsymbol{a}_{vt}$ and $\boldsymbol{a}_{vn}$ = projections on a vertical plane of the tangential and normal components of droplet acceleration, respectively, excluding components of gravitational acceleration (L/T^2); and $\boldsymbol{F}_{\mathrm{WD}}$ = wind drift force $[ML/T^2]$)

projected on the horizontal plane) is partly reflected in the attenuation of droplet absolute velocity ($\boldsymbol{a}_{ht}$) and partly on droplet drift, which is a function of $\boldsymbol{a}_{hn}$.

As is the case with the condition in which wind velocity is considered zero, here as well the projected trajectory of the droplet on the vertical plane represents curvilinear motion (Figure 3c). Hence droplet acceleration on the vertical plane has both tangential and normal components. The tangential component, $\boldsymbol{a}_{vt}$, represents the change in the magnitude of droplet absolute velocity on the vertical plane (taking into account wind effects). The normal component, $\boldsymbol{a}_{vn}$, on the other hand, accounts for the change in direction of the projection of droplet absolute velocity vector on the vertical plane, hence it is responsible for the curvilinear motion there. Note that $\boldsymbol{a}_{vn}$ does not include the component of gravitational acceleration normal to droplet trajectory. It can then be noted that, in contrast to the condition in which there is no wind, herein the normal component of acceleration on the vertical plane is the vector sum of a component due to wind drift effects, $\boldsymbol{a}_{vn}$, and a component of the gravitational acceleration. This implies that wind effect on droplet drift has a vertical component as well.

5.3 Major forces acting on a droplet and equations

Noting that droplet acceleration in a given direction is proportional to the net unbalanced force on the droplet in that same direction, droplet acceleration components shown in Figures 3b and 3c will be used to define the major forces acting on the droplet. It can readily be noted that droplet weight, $\boldsymbol{F}_w$, which is directly proportional to gravitational acceleration, g, is one of the forces that acts on the droplet. It can also be noted that the droplet tangential acceleration, $\boldsymbol{a}_t$ (which is a function of $\boldsymbol{a}_{ht}$ and $\boldsymbol{a}_{vt}$), is evidently related to the attenuation of droplet velocity due to aerodynamic drag as affected by wind, $\boldsymbol{D}$. Considering the preceding discussion on droplet acceleration components it is readily evident that the droplet normal acceleration, in three dimensions, $\boldsymbol{a}_n$ (which is a function of $\boldsymbol{a}_{hn}$ and $\boldsymbol{a}_{vn}$), is directly proportional to the force that wind exerts on the droplet in a direction normal to its absolute velocity vector, henceforth referred to as droplet wind drift force, $\boldsymbol{F}_{WD}$. The relationship between the major forces acting on the droplet is shown in the droplet free-body diagram (Figure 3d). For a droplet undergoing accelerated motion under wind, the net unbalanced force acting on it can then be expressed as the vector sum of drag, droplet weight, and wind drift forces:

$$\sum \boldsymbol{F} = \boldsymbol{D} + \boldsymbol{F_w} + \boldsymbol{F}_{WD} \qquad (32)$$

The equation for approximating aerodynamic drag on a droplet undergoing unsteady motion, $\boldsymbol{D}$, has the same form as that given in Eq. 17, with the recognition that the computation of the relative velocity vector needs to take wind effects into account. The droplet weight, $\boldsymbol{F}_w$, can be readily computed with Eq. 18. On the other hand, the equation for $\boldsymbol{F}_{WD}$ is not obvious. A question arises as to how the wind drift force, $\boldsymbol{F}_{WD}$, can be expressed in terms of droplet mass and the kinematic variables of displacement, time, and velocity.

5.4 Conceptualization of the physical mechanism of wind drift and equations

In order to facilitate subsequent discussion as related to the conceptualization of the physical mechanism of wind drift and the nature of the wind drift force and the derivation of a mathematical expression for $\boldsymbol{F}_{WD}$, a velocity diagram at some instant during droplet motion depicting droplet absolute velocity vector, its projection on a horizontal plane, $\boldsymbol{V}_h(t)$, and the wind velocity vector is presented in Figure 4a. In addition, droplet trajectory in three dimensions with wind velocity vector resolved into its components along the droplet absolute velocity vector, $\boldsymbol{W}_c$, and normal to the droplet absolute velocity vector, $\boldsymbol{W}_n$, is shown in Figure 4b.
It can be noted form the discussion in Sections 5.2 and 5.3 that $\boldsymbol{W}_n$ and $\boldsymbol{W}_c$ are collinear with the droplet normal acceleration, $\boldsymbol{a}_n$, and tangential acceleration, $\boldsymbol{a}_t$, vectors, respectively. It then follows that $\boldsymbol{W}_n$ is related to the wind induced curvilinear droplet motion and hence to the wind drift force and $\boldsymbol{W}_c$ represents wind effects on drag.

Now consider a scenario in which the wind velocity vector, $\boldsymbol{W}$, and the droplet absolute velocity vector, $\boldsymbol{V}$, lie on the same vertical plane ($\alpha_h = 0$), it can then be noted that $\boldsymbol{W}_c$ and $\boldsymbol{W}_n$ (Figure 4b) as well lie on the same vertical plane. In which case, droplet motion would be restricted to the vertical plane containing these vectors and there would be no wind induced droplet motion on the horizontal plane ($\boldsymbol{a}_{hn} = 0$). Wind effects on droplet motion should then be confined to aerodynamic drag and droplet drift on the same vertical plane. Note that such a scenario occurs when the centerline of the sprinkler nozzle and the wind velocity vector are on the same vertical plane at the time droplet is released. It could also occur, at some point during droplet motion, if the angle α_h at the time of droplet release from sprinkler nozzle is sufficiently

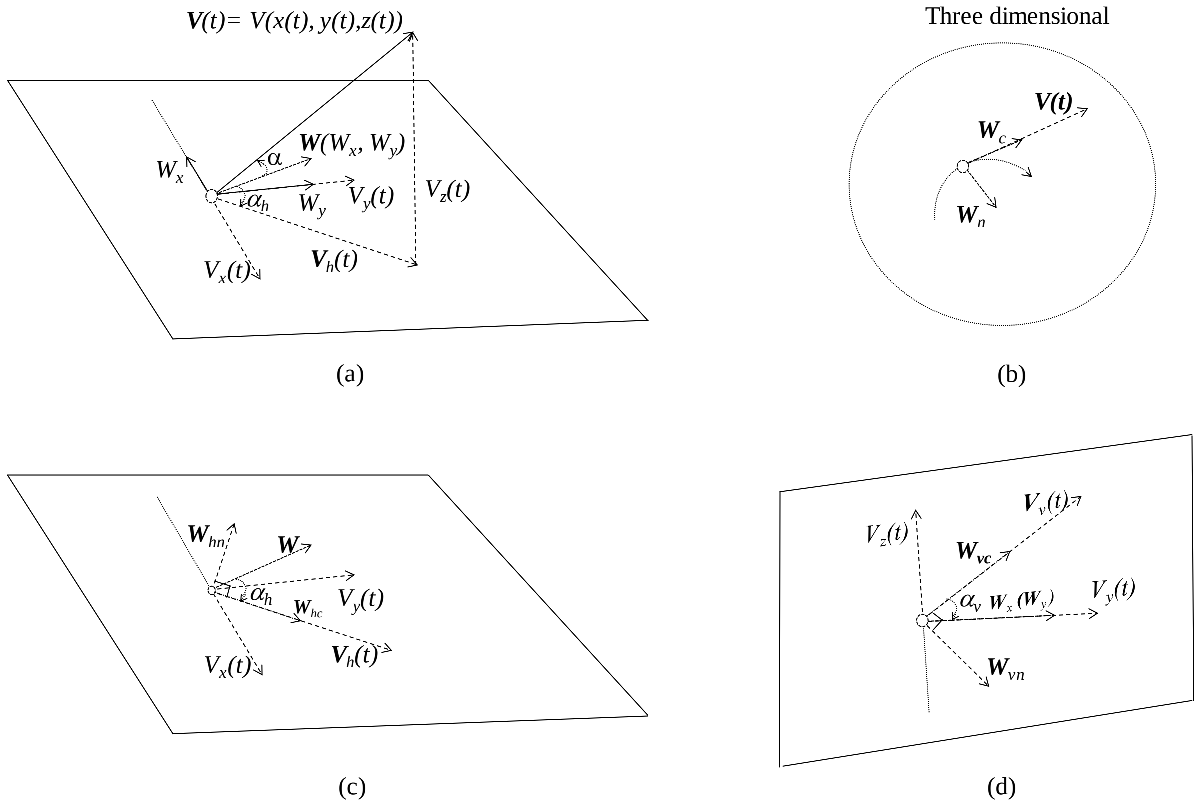

Figure 4 (a) Velocity diagram showing the instantaneous droplet absolute velocity, ***V(t)***, the projection of the droplet absolute velocity vector on the horizontal plane, $\boldsymbol{V}_h$, and the wind velocity vector , ***W***, and their components along the coordinate axes; (b) Droplet absolute velocity vector and the components of the wind velocity vector along and in a direction normal to ***V***: $\boldsymbol{W}_c$ and $\boldsymbol{W}_n$, respectively; (c) Projections of ***V***, $\boldsymbol{W}_c$, and $\boldsymbol{W}_n$ on a horizontal plane: $\boldsymbol{V}_h$, $\boldsymbol{W}_{hc}$, and $\boldsymbol{W}_{hn}$, respectively; and (d) Projections of ***V***, $\boldsymbol{W}_c$, and $\boldsymbol{W}_n$ on a vertical plane: $\boldsymbol{V}_v$, $\boldsymbol{W}_{vc}$, and $\boldsymbol{W}_{vn}$, respectively (Note that the projection of wind velocity vector on the vertical plane is either $\boldsymbol{W}_x$ or $\boldsymbol{W}_y$, depending on the vertical plane considered; α = the angle between droplet absolute velocity vector and wind velocity vector; and α_h = the angle between $\boldsymbol{V}_h$ and wind velocity vector, α_v = the angle $\boldsymbol{V}_v$ makes with the horizontal)

small, for the prevailing wind velocity vector to cause the droplet to veer into a course that its corresponding $\boldsymbol{V}_h$ eventually becomes collinear with the wind velocity vector. A more typical scenario, under field irrigation settings, is one in which the angle between the wind velocity vector and the horizontal projection of the droplet absolute velocity vector is different from zero ($\alpha_h \neq 0$). In which case, the droplet absolute velocity and the wind velocity vectors do not lie on the same vertical plane (or ***V***, $\boldsymbol{V}_h$, and ***W*** are not coplanar). The implication is that the component of the wind velocity vector normal to the droplet absolute velocity vector, $\boldsymbol{W}_n$, does not lie on the same vertical plane as $\boldsymbol{V}$ and $\boldsymbol{V}_h$. In which case its projection on the horizontal plane, $\boldsymbol{W}_{hn}$, is normal to the vertical plane containing $\boldsymbol{V}$ and $\boldsymbol{V}_h$. Figure 4c depicts $\boldsymbol{V}_h$, $\boldsymbol{W}$, and the projections on the horizontal plane of $\boldsymbol{W}_c$ and $\boldsymbol{W}_n$, $\boldsymbol{W}_{hc}$ and $\boldsymbol{W}_{hn}$, respectively. It can be noted that $\boldsymbol{W}_{hn}$ is collinear with $\boldsymbol{a}_{hn}$, hence related to the curvilinear motion of droplet on the horizontal plane and the projection on the horizontal plane of the wind drift force. In which case $\boldsymbol{W}_{hc}$, which is collinear with $\boldsymbol{a}_{ht}$, represents wind effects on aerodynamic drag on the horizontal plane. Similarly, Figure 4d shows the projection on a vertical plane of the droplet absolute velocity vector, $\boldsymbol{V}_v(t)$, the projections on the vertical plane of $\boldsymbol{W}_c$ and $\boldsymbol{W}_n$, $\boldsymbol{W}_{vc}$ and $\boldsymbol{W}_{vn}$, respectively. Here as well the normal component of the wind velocity vector, $\boldsymbol{W}_{vn}$, contributes to the curvilinear motion of droplet on the vertical plane and is collinear with $\boldsymbol{a}_{vn}$, hence related to the projection of the wind drift force on the vertical plane. It then follows that $\boldsymbol{W}_{vc}$ represents the effect of wind on aerodynamic drag on the vertical plane. The preceding discussion shows that droplet wind drift induces a shift in droplet trajectory, compared to an equivalent no-wind condition, both on the horizontal and vertical planes.

While the above discussion helps visualize the effect of wind on droplet motion, eventually a quantitative description of wind effects on droplet motion has to be made in a three dimensional coordinate system (Figure 4b). In subsequent section, some specific observations will be made, on the properties of the wind velocity components of $\boldsymbol{W}_c$ and $\boldsymbol{W}_n$, leading to the conceptualization of the mechanism of droplet wind drift force, $\boldsymbol{F}_{WD}$, and the derivation of an approximate equation for $\boldsymbol{F}_{WD}$:

(i) Considering that the angle between the droplet absolute velocity vector and wind velocity vector, α, vary with droplet spatial coordinates and hence time (Figure 4a), it then follows that the relative magnitudes of the components of $\boldsymbol{W}$ along and in a direction normal to $\boldsymbol{V}$ (i.e., $\boldsymbol{W}_c$ and $\boldsymbol{W}_n$) should vary as a function of droplet spatial coordinate as well.

(ii) Noting that $\boldsymbol{W}_n$ is normal to $\boldsymbol{V}$ and collinear with the normal droplet acceleration, $\boldsymbol{a}_n$, and hence with the wind drift force, $\boldsymbol{F}_{WD}$; it can be noted that $\boldsymbol{W}_n$ is the component of the wind velocity vector that is related to the droplet wind drift force: $F_{WD} \propto W_n$.

(iii) It then follows that the $\boldsymbol{W}_c$ vector (which is collinear with droplet absolute velocity vector $\boldsymbol{V}$ and the tangential acceleration, $\boldsymbol{a}_t$) is the component of the wind velocity vector that represents the effect of wind on aerodynamic drag. Hence only a component of the relative velocity vector, hereafter referred to as $\boldsymbol{V}_r{}'$ (and is given as $\boldsymbol{V}_r{}' = \boldsymbol{V}-\boldsymbol{W}_c$) would be used to compute aerodynamic drag.

(iv) If a mathematical expression can be derived for $\boldsymbol{W}_c$, then the equation for computing $\boldsymbol{V}_r{}'$ follows, based on which the drag force can be computed. As will be shown subsequently, an equation can be derived for $\boldsymbol{W}_c$ as a function of $\boldsymbol{W}$ and $\boldsymbol{V}(t)$ vectors based on vector algebra. Note that an expression for $\boldsymbol{W}_n$ can then be obtained in terms of $\boldsymbol{W}$ and $\boldsymbol{W}_c$.

The preceding observations would be used to conceptualize the nature and mechanism of wind drift force, $\boldsymbol{F}_{WD}$, and to derive a mathematical expression for it. In addition, equations for $\boldsymbol{W}_c$, $\boldsymbol{W}_n$, and $\boldsymbol{V}_r{}'$ will be derived and the drag force equation will be defined in light of the expression obtained for $\boldsymbol{V}_r{}'$.

Equation for $\boldsymbol{F}_{WD}$: Having shown that there exists a relationship between $\boldsymbol{F}_{WD}$ and $\boldsymbol{W}_n$, the form of the equation that relates $\boldsymbol{F}_{WD}$ with $\boldsymbol{W}_n$ would follow if only the nature of $\boldsymbol{F}_{WD}$ can be defined. Intuitive physical reasoning suggests that the wind drift force, $\boldsymbol{F}_{WD}$, can be conceived as a pressure force that the flowing ambient air mass exerts on the droplet in a direction normal to droplet trajectory. In which case, a function with the same form as Eq. 15 can be used to compute the force acting on the droplet. Noting that $\boldsymbol{V}$ and $\boldsymbol{W}_n$ are orthogonal, it follows that the droplet relative velocity with respect to the ambient air in a direction normal to $\boldsymbol{V}$ is equal to $-\boldsymbol{W}_n$. The modulus of the wind drift force can then be expressed, with an equation of the form similar to Eq. 15, as follows

$$|\boldsymbol{F}_{WD}| = C_{WD} A \frac{\rho}{2} |\boldsymbol{W}_n|^2 \qquad (33)$$

The vector form of which is given as

$$\boldsymbol{F}_{WD} = C_{WD} A \frac{\rho}{2} |\boldsymbol{W}_n| \boldsymbol{W}_n \qquad (34)$$

where C_{DW} = empirical coefficient for the wind drift force equation, could be expressed as some function of the unsteady drag coefficient, C_{du}. The preceding discussion shows that if the equations for $\boldsymbol{W}_c$ and $\boldsymbol{W}_n$ are given, aerodynamic drag and wind drift forces acting on a droplet can be computed with equations 15 and 34, respectively. In what follows vector algebra will be used to derive expressions for $\boldsymbol{W}_c$ and $\boldsymbol{W}_n$ in terms of the wind velocity and the droplet absolute velocity vectors.

Equation for $\boldsymbol{W_c}$: Noting that $\boldsymbol{W}_c$ is the projection of $\boldsymbol{W}$ on $\boldsymbol{V}$ (Figure 4d) and using the formula for the scalar product of vectors, the modulus of $\boldsymbol{W}_c$ can be expressed as

$$|\boldsymbol{W}_c| = |\boldsymbol{W}| \frac{\boldsymbol{W} \bullet \boldsymbol{V}}{|\boldsymbol{W}||\boldsymbol{V}|} = \frac{\boldsymbol{W} \bullet \boldsymbol{V}}{|\boldsymbol{V}|} \tag{35}$$

where $|\bullet|$ = the modulus of a vector and $\boldsymbol{W} \bullet \boldsymbol{V}$ = the dot (scalar) product of $\boldsymbol{W}$ and $\boldsymbol{V}$. Noting that the vector equations for $\boldsymbol{W}$ and $\boldsymbol{V}$ in a rectangular coordinate system can be given as

$$\boldsymbol{W} = W_x\boldsymbol{i} + W_y\boldsymbol{j} \quad and \quad \boldsymbol{V} = V_x\boldsymbol{i} + V_y\boldsymbol{j} + V_z k \tag{36}$$

The equations for $\boldsymbol{W}_c$ can be given as

$$\boldsymbol{W}_c = \frac{\boldsymbol{W} \bullet \boldsymbol{V}}{|\boldsymbol{V}|^2}\boldsymbol{V} = (V_x\delta)\boldsymbol{i} + (V_y\delta)\boldsymbol{j} + (V_z\delta)k \tag{37}$$

In Eq. 37 δ is given as

$$\delta = \frac{\boldsymbol{W} \bullet \boldsymbol{V}}{|\boldsymbol{V}|^2} = \frac{W_xV_x + W_yV_y}{V_x^2 + V_y^2 + V_z^2} \tag{38}$$

The component of the droplet relative velocity vector, $\boldsymbol{V}_r'$, that would be used to compute the drag force, $\boldsymbol{D}$ (Eq. 15), is given as:

$$\boldsymbol{V}_r' = \boldsymbol{V} - \boldsymbol{W}_c = V_{rx}\boldsymbol{i} + V_{ry}\boldsymbol{j} + V_{rz}\boldsymbol{k} \tag{39}$$

where V_{rx}, V_{ry}, and V_{rz} are given as

$$V_{rx} = V_x(1-\delta), \quad V_{ry} = V_y(1-\delta), \quad and \quad V_{rz} = V_z(1-\delta) \tag{40}$$

Equation for $\boldsymbol{W_n}$: The wind velocity vector, $\boldsymbol{W}$, is the vector sum of $\boldsymbol{W}_n$ and $\boldsymbol{W}_c$ (Figure 4d), hence the modulus of $\boldsymbol{W}_n$ can readily be obtained in terms of the wind velocity vector, $\boldsymbol{W}$, and $\boldsymbol{W}_c$

$$|\boldsymbol{W}_n| = \sqrt{|\boldsymbol{W}|^2 - |\boldsymbol{W}_c|^2} \tag{41}$$

The equation for $\boldsymbol{W}_n$ can then be expressed as

$$\boldsymbol{W}_n = \boldsymbol{W} - \boldsymbol{W}_c = \boldsymbol{W} - \frac{\boldsymbol{W} \bullet \boldsymbol{V}}{|\boldsymbol{V}|^2}\boldsymbol{V} \tag{42}$$

The vector form of $\boldsymbol{W}_n$ can be given as

$$\boldsymbol{W}_n = \boldsymbol{W} - \boldsymbol{W}_c = (W_x - V_x\delta)\boldsymbol{i} + (W_y - V_y\delta)\boldsymbol{j} + (-V_z\delta)\boldsymbol{k} \tag{43}$$

Note that Eq. 34 can be used to evaluate the wind drift force acting on the droplet, $\boldsymbol{F}_{WD}$, with $\boldsymbol{W}_n$ defined in accordance with Eq. 43.

5.5 Equation of droplet dynamics under wind

It follows from the preceding discussion that the vector sum of forces acting on a droplet undergoing an impulsively started accelerated motion under wind can be expressed as

$$\sum \boldsymbol{F} = -C_D A \frac{\rho}{2} |\boldsymbol{V}_r'| \boldsymbol{V}_r' + C_{WD} A \frac{\rho}{2} |\boldsymbol{W}_n| \boldsymbol{W}_n - mg\boldsymbol{k} \tag{44}$$

with $\boldsymbol{V}_r'$ and $\boldsymbol{W}_n$ defined in terms of Eqs. 39 and 43. In Eq. 44, C_D = a coefficient that can be expressed as some empirical function of the unsteady drag coefficient, C_{du}. A possible form of the unsteady drag coefficient will be defined in a subsequent section (Section 6). The equation of motion expressed in vector differential form can then be given as

$$m\left(\frac{d^2x}{dt^2}\boldsymbol{i} + \frac{d^2y}{dt^2}\boldsymbol{j} + \frac{d^2z}{dt^2}\boldsymbol{k}\right) = -C_D A \frac{\rho}{2} |\boldsymbol{V}_r'| \boldsymbol{V}_r' + C_{WD} A \frac{\rho}{2} |\boldsymbol{W}_n| \boldsymbol{W}_n - mg\boldsymbol{k} \tag{45}$$

Equation 45 can be recast as an equivalent set of scalar differential equations along each of the coordinate axes, resulting in six equations with six unknowns

$$\frac{dV_x}{dt} = -\xi C_D \left|\mathbf{V}_r'\right| V_{rx} + \xi C_{WD} \left|\mathbf{W}_n\right| \left(W_x - V_x \delta\right) \qquad (46)$$

$$\frac{dx}{dt} = V_x \qquad (47)$$

$$\frac{dV_y}{dt} = -\xi C_D \left|\mathbf{V}_r'\right| V_{ry} + \xi C_{WD} \left|\mathbf{W}_n\right| \left(W_y - V_y \delta\right) \qquad (48)$$

$$\frac{dy}{dt} = V_y \qquad (49)$$

$$\frac{dV_z}{dt} = -\xi C_D \left|\mathbf{V}_r'\right| V_{rz} - \xi C_{WD} \left|\mathbf{W}_n\right| \left(V_z \delta\right) - g \qquad (50)$$

$$\frac{dz}{dt} = V_z \qquad (51)$$

Problem definition is complete with the statement of initial conditions (Eq. 30). The system of nonlinear differential equations (Eqs. 46-51) coupled with the initial conditions can be solved numerically. Equations 46-51 describe a more general form of an impulsively started accelerated motion of water droplet that occurs under a steady uniform horizontal wind. It can be shown that the form of the equations derived for no wind condition, Eqs. 22-27, represent a special case of Eqs. 46-51 obtained by setting the wind velocity vector to zero.

Note that Eqs. 46-51 were not used in developing the numerical droplet dynamics model that forms the basis of the sprinkler irrigation precipitation pattern simulation model presented in subsequent sections and in the companion document. The reason was that the above set of equations were derived after the numerical model, described subsequently, is developed based on approximate forms of the governing equations of droplet dynamics. However, it is included here as part of the background theoretical review and development conducted within the framework of the study reported here. In what follows the approximate formulation of the droplet dynamics equations, which was solved numerically and forms the physical basis of the sprinkler precipitation pattern simulation model developed in this study is presented.

Chapter 6 Numerical droplet dynamics model developed as part of the current study

6.1 Review and derivation of equations

Derivation of the equations that form the basis of the droplet dynamics model developed as part of the current study combines established ideas proposed in earlier studies and also new concepts formulated as part of the current study in the preceding sections (Section 5). Sprinkler irrigation is typically undertaken under wind condition and droplet dynamics under no-wind condition is a special case of that occurring under wind. Hence, the general case of droplet motion under wind is considered here, which is unsteady and curvilinear. A discussion on the forces that the ambient air exerts on a droplet undergoing unsteady motion and the modification that need to be made to the steady state drag coefficient in order to take into account the aggregate effects of the various forces in the drag equation is described in Section 3. In addition, the discussion in Section 5 have also shown that the major forces acting on a droplet undergoing unsteady motion under wind consists of drag, droplet weight, and wind drift force. However, as an initial approximation, here wind effects on drag and droplet drift are assumed to be encapsulated in the drag equation. Note that this is consistent with the approach commonly used in sprinkler irrigation droplet dynamics modeling (Fukui et al., 1980; Vories et al., 1987; Seginer et al., 1991; Carrion et al., 2001, Playan et al., 2009). In which case, the aerodynamic drag force, $\boldsymbol{D}$, can be expressed with an equation of the form given in Eq. 15. As can be noted form Figure 5, with this formulation the variable $\boldsymbol{V}_r$ is equal to the relative velocity vector, given as

$$\boldsymbol{V}_r = \boldsymbol{V} - \boldsymbol{W} = (V_x - W_x)\boldsymbol{i} + (V_y - W_y)\boldsymbol{j} + V_z\boldsymbol{k} \tag{52}$$

Substituting Eq. 52 in Eq. 15 yields the drag equation

$$\boldsymbol{D} = -C_{du} A \frac{\rho}{2} |\boldsymbol{V}_r| \left((V_x - W_x)\boldsymbol{i} + (V_y - W_y)\boldsymbol{j} + V_z\boldsymbol{k} \right) \tag{53}$$

With the drag force expressed in terms of Eq. 53, the resulting system of equations for describing droplet motion has the same form as that of Eqs. 22-27, with the exception that $\boldsymbol{V}_r$ here is different from droplet absolute velocity. Evidently the simplicity of this system of equations and its amenability to numerical solution with widely used techniques (Burden et al., 1981; Press et al., 1997; Matthews et al., 2004) are advantages. However, the numerical solutions of these

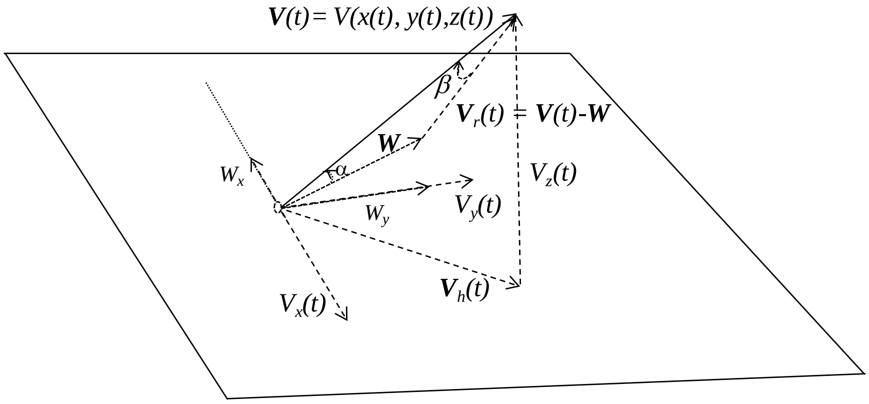

Figure 5 Velocity diagram depicting droplet absolute velocity, wind velocity vector, and the relative velocity vector (where α = angle between wind velocity and droplet absolute velocity vector and β = angle between droplet absolute and relative velocity vectors)

equations do not reproduce wind effects adequately, hence, approaches that modify Eq. 53 to better approximate wind effects have been proposed (e.g., Seginer et al., 1991; Carrion et al. 2001; Playan et al., 2009). These formulations generally aim at deriving approximate expressions for the effect of wind on both drag and droplet drift using a form of Eq. 53 itself, with the unsteady drag coefficient expressed as a function of the steady state drag coefficient and trigonometric terms implicitly accounting for drag and droplet drift effects.

In subsequent derivation of the equations used in the development of the model presented here, the approach described above will be used with some modifications. The assumption here is that Eq. 53 has the mathematical structure to encapsulate wind effects on both drag and droplet drift, hence when coupled with the expression for droplet weight it can produce the kind of motion resulting from the action of such forces on a droplet in some scaled fashion. Note that the similarity in form of the terms representing aerodynamic drag and wind drift forces on droplets (Eqs. 15 and 34), lends some support to this observation. Accordingly in the model described here, the modification to Eq. 53 consists of resolving the drag force computed with Eq. 53 into a component collinear with the droplet absolute velocity vector, $\boldsymbol{D}'$, which represents the effect of wind on drag and into a component normal to the droplet absolute velocity vector, $\boldsymbol{F}_{WD}'$, which approximates the effect of wind on droplet drift. From vector algebra it can be shown that

$$\boldsymbol{D}' = |\boldsymbol{D}| \frac{\boldsymbol{D} \bullet \boldsymbol{V}}{|\boldsymbol{D}||\boldsymbol{V}|} \frac{\boldsymbol{V}}{|\boldsymbol{V}|} = \frac{\boldsymbol{D} \bullet \boldsymbol{V}}{|\boldsymbol{V}|^2} \boldsymbol{V} \qquad (54)$$

which can be expressed as

$$\boldsymbol{D}' = (\psi_1 \boldsymbol{V}_r \bullet \boldsymbol{V})\boldsymbol{V} \quad \textit{where} \quad \psi_1 = -C_{du} A \frac{\rho}{2} \frac{|\boldsymbol{V}_r|}{|\boldsymbol{V}|^2} \qquad (55)$$

In terms of the components of droplet absolute velocity and wind velocity vectors, along the coordinate axes, we have:

$$\boldsymbol{D}' = \psi_2 (V_x \boldsymbol{i} + V_y \boldsymbol{j} + V_z \boldsymbol{k}) \qquad (56)$$

where

$$\psi_2 = \psi_1 \left(V_x (V_x - W_x) + V_y (V_y - W_y) + V_z^2 \right) \qquad (57)$$

Noting that $\boldsymbol{D}'$ computed as such is not the exact expression for drag, Eq. 56 is multiplied by a scale factor, ζ_1:

$$\boldsymbol{D}' = \zeta_1 \psi_2 (V_x \boldsymbol{i} + V_y \boldsymbol{j} + V_z \boldsymbol{k}) \qquad (58)$$

Now an expression will be derived for the component of the drag force, $\boldsymbol{D}$, normal to the droplet absolute velocity vector, which is used as a surrogate for the wind drift force, $\boldsymbol{F}_{WD}'$. Noting that the drag force, $\boldsymbol{D}$ (Eq. 53), is the vector sum of $\boldsymbol{D}'$ (Eq. 56) and $\boldsymbol{F}_{WD}'$, we have

$$\boldsymbol{F}_{WD}' = \boldsymbol{D} - \boldsymbol{D}' = \boldsymbol{D} - (\psi_1 \boldsymbol{V}_r \bullet \boldsymbol{V})\boldsymbol{V} \qquad (59)$$

This can be expressed in terms of the components of the droplet absolute velocity vector and the wind velocity vector along the coordinate axes as follows:

$$\boldsymbol{F}_{WD}' = (\psi (V_x - W_x) - \psi_2 V_x)\boldsymbol{i} + (\psi (V_y - W_y) - \psi_2 V_y)\boldsymbol{j} + \psi_3 V_z \boldsymbol{k} \qquad (60)$$

where

$$\psi = -C_{du} A \frac{\rho}{2} |\boldsymbol{V}_r| \quad \textit{and} \quad \psi_3 = \psi - \psi_2 \qquad (61)$$

Noting that $\boldsymbol{F}_{WD}'$ computed as such is not the exact expression for wind drift force, Eq. 60 is multiplied by a scale factor, ζ_2:

$$\boldsymbol{F}_{WD}' = \zeta_2 \left[\left(\psi (V_x - W_x) - \psi_2 V_x \right) \boldsymbol{i} + \left(\psi (V_y - W_y) - \psi_2 V_y \right) \boldsymbol{j} + \psi_3 V_z \boldsymbol{k} \right] \qquad (62)$$

As described in a preceding discussion (Section 3.2), the effect of acceleration on droplet motion is taken into account by replacing the steady state drag coefficient with the unsteady drag coefficient. Temkin and Kim (1980) and Temkin and Mehta (1982) proposed an empirical expression for the unsteady drag coefficient given as the sum of the steady state drag coefficient and a term representing some function of the droplet acceleration number. The equation was developed based on laboratory experiments covering limited set of conditions in terms of droplet *Re*, droplet diameter ranges, and air flow velocity compared to those encountered in field sprinkler applications. Hence, the applicability of their equation to droplet motion in field sprinkler irrigation modeling context is yet to be determined. In the model developed here the effect of acceleration is taken into account by introducing an empirical drag correction parameter for acceleration effects, ζ_3, in a form given in Eq. 63

$$C_{du} = C_{ds}(Re) + \zeta_3 \qquad (63)$$

Substituting Eqs. 18, 58, and 62, in Eq. 32 yields the expression for the vector sum of forces acting on the droplet

$$\sum \boldsymbol{F} = \zeta_1 \psi_2 \left(V_x \boldsymbol{i} + V_y \boldsymbol{j} + V_z \boldsymbol{k} \right) + \zeta_2 \begin{pmatrix} \left(\psi (V_x - W_x) - \psi_2 V_x \right) \boldsymbol{i} \\ + \left(\psi (V_y - W_y) - \psi_2 V_y \right) \boldsymbol{j} + \psi_3 V_z \boldsymbol{k} \end{pmatrix} - mg\boldsymbol{k} \qquad (64)$$

From Eq. 9, the vector differential equation describing droplet motion can then be given as

$$m \left(\frac{d^2 x}{dt^2} \boldsymbol{i} + \frac{d^2 y}{dt^2} \boldsymbol{j} + \frac{d^2 z}{dt^2} \boldsymbol{k} \right) = \zeta_1 \psi_2 \left(V_x \boldsymbol{i} + V_y \boldsymbol{j} + V_z \boldsymbol{k} \right)$$
$$+ \zeta_2 \begin{pmatrix} \left(\psi (V_x - W_x) - \psi_2 V_x \right) \boldsymbol{i} \\ + \left(\psi (V_y - W_y) - \psi_2 V_y \right) \boldsymbol{j} + \psi_3 V_z \boldsymbol{k} \end{pmatrix} - mg\boldsymbol{k} \qquad (65)$$

The corresponding scalar differential equations are

$$\frac{dV_x}{dt} = \lambda_1 (V_x - W_x) + \lambda_2 V_x \qquad (66)$$

$$\frac{dx}{dt} = V_x \qquad (67)$$

$$\frac{dV_y}{dt} = \lambda_1 (V_y - W_y) + \lambda_2 V_y \qquad (68)$$

$$\frac{dy}{dt} = V_y \qquad (69)$$

$$\frac{dV_z}{dt} = \lambda_3 V_z - g \qquad (70)$$

$$\frac{dz}{dt} = V_z \qquad (71)$$

where

$$\lambda_1 = \zeta_2 \psi \psi_4 \qquad (72)$$

$$\lambda_2 = \psi_2 \psi_4 (\zeta_1 - \zeta_2) \qquad (73)$$

$$\lambda_3 = (\zeta_1 \psi_2 + \zeta_2 \psi_3) \psi_4 \qquad (74)$$

where ψ_4 = the reciprocal of droplet mass (1/*M*). Equations 66-71 represent a coupled system of (six) ordinary differential equations with six variables, which constitute an initial value problem that can be solved numerically given the initial conditions (Eq. 31). The numerical solution of this system of equations is described by Zerihun and Sanchez (2014).

The model parameters defined above, Eqs.58, 62, and 63, are scale factors for wind effects on drag, ζ_1, and droplet drift, ζ_2, and the drag coefficient correction factor for acceleration effects, ζ_3. These parameters can in theory be estimated through inverse modeling, if all the model inputs including initial conditions and wind velocity vector are known and the complete trajectory of a droplet is given. Although some physical meaning (scale factors and drag correction parameters for acceleration effects) can be attributed to these parameters when used in droplet dynamics modeling context, when applied to sprinkler irrigation precipitation pattern simulation they are simple shape fitting parameters. The range of variation of these parameters is not yet determined. However, under some special conditions the above equations reduce to simpler forms. Parameter values pertinent to this conditions and tentative ranges obtained based on numerical simulations are described in the main report of this study.

References

Aggarwal, S.K., and Peng, F. (1995). A review of droplet dynamics and vaporization modeling for engineering calculations. *J. Eng. Gas Turbines and Power*, ASME, 117:453-461.

Arya, S.P. (1988). *Introduction to micrometrology*. Academic Press Inc. New York, NY.

Burden, L.R., Fairies, J.D., and Reynolds, A.C. (1981). *Numerical analysis*. Prindle, Weber, & Schmidt, Boston, MA.

Carrion, P. Tarjuelo, J.M., Montero, J. (2001). SIRIAS: a simulation model for sprinkler Irrigation, I. Description. *Irrig. Sci.* (2001)20:73-84.

Fukui, Y., Nakanishi, K., and Okamura, S. (1980). Computer simulation of sprinkler irrigation uniformity. *Irrig. Sci.*, (1980)2:23-32.

Granger, R.A. (1995). *Fluid Mechanics*. Dover Publications Inc., New York, NY.

Karanfilian, S.K. and Kotas, T.J. (1978). Drag on a sphere in unsteady motion in a liquid at rest. *J. Fluid Mech*, 87(1):85-96.

Langhaar, H.L. 1980. *Dimensional analysis and theory of models.* Robert E. Kreiger Publishing Company, Huntington, NY.

Laws, J.O. (1941). Measurement of the fall velocity of water-drops and raindrops. *Trans Am. Geophys. Union*, (22):709-721.

Mathews, J.M. and Fink, K.D. (2004). *Numercial methods using Matlab*. Prentice Hall Inc., Upper Saddle River, NJ.

Odar, F and Hamilton, W.S. (1964). Forces on a sphere accelerating in a viscous fluid. *J. Fluid Mech* 18:302-314.

Playan, E., Burguete, J., Zapata, N., Salvador, R., Bautista-Capetillo, C., Cavero, J. Martinez-Cob, A., Faci, J. and Dechmi, F. (2009). Mathematical problems and solutions in sprinkler irrigation. *Monografias de la Real Academia de Ciencias de Zaragoza*, 31:153-174.

Press, W.H., Teukolsky, S.A, Vetterling, W.T., and Flannery, B.P (1997). *Numercial Recipes in C, the art of scientific computing*. Cambridge University Press, New York, NY.

Seginer, I., Nir, D., von Bernuth, R.D. (1991). Simulation of wind distorted sprinkler patterns. *J. Irrig. Drain Eng.*, ASCE, 117(2):285-306.

Shames, I.H. (1966). *Engineering Mechanics, Vol. II: Dynamics*. Prentice-Hall Inc., Englewood Cliffs, NJ.

Soutas-Little, R.W. and Inman, D.J. (1999). *Engineering mechanics, Dynamics*. Prentice-Hall, Inc., Upper saddle river, NJ.

Temkin, S. and Kim, S.S. (1980). Droplet motion induced by weak shock waves. *J. Fluid Mech*, 96(1):133-157.

Temkin, S. and Mehta, H.K. (1982). Droplet drag in accelerating and decelerating flow. *J. Fluid Mech* (116):297-313.

Vennard, J.K. (1941). *Elementary fluid mechanics*. John Willey & Sons, Inc., New York, NY.

von Bernuth, R.D. and Gilley, J.R. (1984). Sprinkler droplet size distribution estimation from single leg test data. *Trans.* ASAE, 27(5):1435-1141.

Vories, E.D., von Bernuth, R.D., and Michelson, R.H. (1987). Simulating sprinkler performance in wind. *J. Irrig Drain Eng.*, ASCE, 113(1):119-130.

Zerihun, D. and Sanchez, C.A. (2014). Sprinkler irrigation precipitation pattern simulation model: Development and evaluation. *A report submitted to the* USBR.